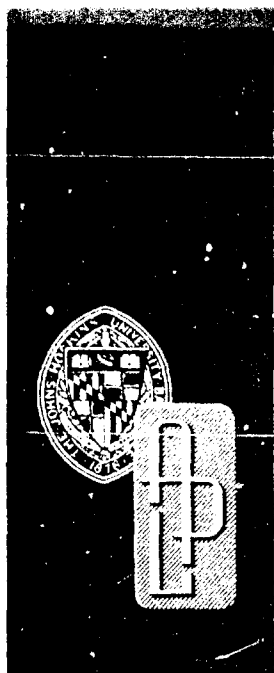


APL/JHU

TG 1291

MARCH 1976

Copy No. 7



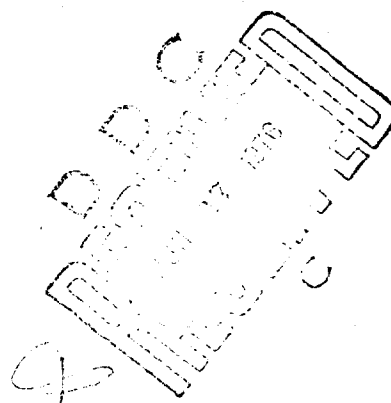
1.2

AD A025714

*Technical Memorandum*

# **TROPOSPHERIC EFFECTS ON SIGNALS AT VERY LOW ELEVATION ANGLES**

by H. S. HOPFIELD



**BEST AVAILABLE COPY**

THE JOHNS HOPKINS UNIVERSITY - APPLIED PHYSICS LABORATORY

APL/JHU  
TG 1291  
MARCH 1976

*Technical Memorandum*

**TROPOSPHERIC EFFECTS  
ON SIGNALS AT  
VERY LOW ELEVATION ANGLES**

by H. S. HOPFIELD

THE JOHNS HOPKINS UNIVERSITY ■ APPLIED PHYSICS LABORATORY  
Johns Hopkins Road • Laurel, Maryland • 20810  
Operating under Contract N00017-72-C-4401 with the Department of the Navy

Approved for public release, distribution unlimited

## REPORT DOCUMENTATION PAGE

1. REPORT NUMBER 14 APL/JHU/TC-1291	2. GOVT ACCESSION NO	3. RECIPIENT'S CATALOG NUMBER 9
4. TITLE (and Subtitle) 6 TROPOSPHERIC EFFECTS ON SIGNALS AT VERY LOW ELEVATION ANGLES	5. TYPE OF REPORT & PERIOD COVERED Technical Memorandum	
7. AUTHOR(s) 10 Helen S. Hopfield	8. CONTRACT OR GRANT NUMBER(s) 15 N00017-72-C-4401	6. PERFORMING ORG. REPORT NUMBER TG 1291
9. PERFORMING ORGANIZATION NAME & ADDRESS The Johns Hopkins University Applied Physics Laboratory Johns Hopkins Rd. Laurel, MD 20810	10. PROGRAM ELEMENT, PROJECT, TASK AREA & WORK UNIT NUMBERS 12 407.	
11. CONTROLLING OFFICE NAME & ADDRESS Defense Mapping Agency Topographic Center Washington, DC 20315	12. REPORT DATE 11 Mar 76	13. NUMBER OF PAGES 44
14. MONITORING AGENCY NAME & ADDRESS Naval Plant Representative Office 8621 Georgia Ave. Silver Spring, MD 20910	15. SECURITY CLASS. (of this report) Unclassified	
16. DISTRIBUTION STATEMENT (of this Report) Approved for public release; distribution unlimited.	15a. DECLASSIFICATION/DOWNGRADING SCHEDULE	
17. DISTRIBUTION STATEMENT (of the abstract entered in Block 20, if different from Report)		
18. SUPPLEMENTARY NOTES		
19. KEY WORDS (Continue on reverse side if necessary and identify by block number) tropospheric range error      satellite signals      low elevation angles signal path bending      refraction      refraction refractivity      tropospheric range error      radio signal propagation		
20. ABSTRACT (Continue on reverse side if necessary and identify by block number) Two possible sources of error in computing a tropospheric range correction from a model are a mismatch between the model and the actual refractivity profile, and neglect of a signal path bending. To study the error sources, the tropospheric range effect on a radio signal has been evaluated at different elevation angles, for some observed atmospheres, by three methods: (a) using meteorological balloon data, the effect is evaluated along the computed, curved signal path (this is our best estimate of the true effect and is the standard for comparison); (b) using meteorological balloon data, the effect is evaluated for assumed straight-line propagation; and (c) using only surface meteorological data, the effect is evaluated from the two-quartic tropospheric model for assumed straight-line propagation. The differences ((b) - (a)) and ((c) - (b)), respectively, represent the path-bending component and the profile-mismatch component of the total model error ((c) - (a)). Results are presented in figures. The effect of the model-based correction on the computation of tracking-station position is shown for a few sample cases.		

DD FORM 1473  
1 JAN 72

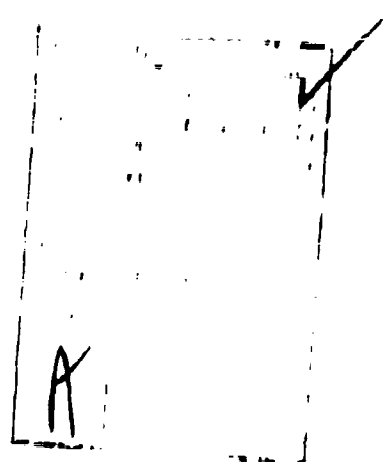
031 650

Unclassified

SECURITY CLASSIFICATION OF THIS PAGE

## CONTENTS

	List of Illustrations . . . . .	5
1.	Introduction and Background . . . . .	7
2.	Theoretical Considerations . . . . .	10
	Procedures for Studying Low-Angle Effects . . . . .	10
	Signal Path Bending . . . . .	12
3.	Numerical Results . . . . .	17
	Ray Tracing . . . . .	17
	Model Predictions at Low Angles . . . . .	23
	Effect of Tropospheric Correction on Station Position . . . . .	33
4.	Summary of Present Status and Future Plans . . . . .	37
	Updating the Data Base . . . . .	37
	More Ray-Tracing Studies . . . . .	38
	More Navigation Studies . . . . .	38
	Acknowledgment . . . . .	39
	References . . . . .	41



# ILLUSTRATIONS

1	Signal Path through the Atmosphere . . . . .	11
2	Mean Tropospheric Range Effect on a Radio Measurement at Oblique Angles . . . . .	18
3	Effect of Signal Path Bending on Radio Range Measurement, $\Delta\rho_{st. line} - \Delta\rho_{curve}$ . . . . .	19
4	Cumulative Angular Bending of Radio Signal Path versus Height above the Earth . . . . .	19
5	Radius of Curvature of Radio Signal Path versus Height Above the Earth . . . . .	20
6	Cumulative Angular Bending of Radio Signal Path versus Refractivity along the Path . . . . .	22
7	Total Angular Bending of Signal Path versus Surface Refractivity . . . . .	23
8	Range Effect of Signal Path Bending versus Surface Refractivity . . . . .	24
9	Optical Signal Path Bending, Theoretical and Ray Traced . . . . .	26
10	Radio Signal Path Bending, Theoretical and Ray Traced . . . . .	27
11	Effect of Path Bending on Radio Range, versus Bending Angle . . . . .	28
12	Range Effect Difference for Radio Signal, $\Delta\rho_{model} - \Delta\rho_{st. line}$ , January 1967 . . . . .	29
13	Range Effect Difference for Radio Signal, $\Delta\rho_{model} - \Delta\rho_{st. line}$ , July 1967 . . . . .	29
14	Total Error in Model Estimate of Tropospheric Effect, $\Delta\rho_{model} - \Delta\rho_{curve}$ for Radio Signal, January 1967 . . . . .	31
15	Total Error in Model Estimate of Tropospheric Effect, $\Delta\rho_{model} - \Delta\rho_{curve}$ for Radio Signal, July 1967 . . . . .	32
16	Effect of Tropospheric Refraction on Apparent Tracking Station Position, Winter Harbor, Maine . . . . .	34
17	Effect of Tropospheric Refraction on Apparent Tracking Station Position, Wahiawa, Hawaii . . . . .	35

## 1. INTRODUCTION AND BACKGROUND

Tropospheric effects on satellite range data, and the difficulty in predicting them, are greater at low elevation angles than at high because of the increased length of the signal path in air, especially in the lower layers of air. The apparent electromagnetic range to a satellite is  $\int n ds$  along the signal path, where  $s$  is the signal path length and  $n$  is the index of refraction of the medium and varies along the path. The atmospheric effect on the measurement is

$$\Delta \rho_{\text{curve}} = \int n ds - \rho, \quad (1)$$

where  $\rho$  is the slant range. If there is no significant curvature of the path, the integral can be taken along the slant range vector and the effect can be written

$$\Delta \rho_{\text{st. line}} = \int (n - 1) d\rho. \quad (2)$$

For convenience, the refractivity ( $N$ ) is defined as

$$N = 10^6(n - 1). \quad (3)$$

A detailed knowledge of the refractivity profile at the pertinent time or a suitable model of it is necessary to evaluate Eqs. (1) or (2) and so to correct for the tropospheric effect. Detailed knowledge of the profile is seldom available. Any reasonable model can be adjusted to give the proper integral of Eq. (2) at the zenith, but only a model that also gives the correct profile shape will give the correct integral of Eq. (2) at both high and low angles. The effect predicted by the two-quartic refractivity profile model,  $\Delta \rho_{\text{model}}$ , will be compared with  $\Delta \rho_{\text{curve}}$  and  $\Delta \rho_{\text{st. line}}$ .

Path bending and model inaccuracy have greater effects near the horizon than at high angles. This study examines both of these low-angle effects.

Refractivity is a function of meteorological conditions. Smith and Weintraub (Ref. 1) give the following expression, for radio frequencies up to at least 15 GHz:

---

Ref. 1. E. K. Smith, Jr., and S. Weintraub, "The Constants in the Equation for Atmospheric Refractive Index at Radio Frequencies." Proc. I.R.E., Vol. 41, No. 8, August 1953, pp. 1035-1057.

$$N = \frac{77.6}{T} \left( P + \frac{4810e}{T} \right) \quad (4)$$

Here  $T$  is the Kelvin temperature, and  $P$  is the total pressure and  $e$  the partial pressure of water vapor, both in millibars. The above two terms of  $N$  are the "dry" and "wet" terms, respectively (subscripts  $d$  and  $w$ ). The two-quartic refractivity profile expression was developed from a study of meteorological balloon data. It deals separately with the height variation of the two terms. The full expression is (Ref. 2):

$$\begin{aligned} N &= N_d + N_w \\ N_d &= \frac{N_{ds}}{(h_d - h_s)^4} (h_d - h)^4 & h \leq h_d \\ N_w &= \frac{N_{ws}}{(h_w - h_s)^4} (h_w - h)^4 & h \leq h_w \end{aligned} \quad (5)$$

In these equations,  $h$  is height above the geoid and the subscript  $s$  refers to surface values. The heights  $h_d$  and  $h_w$  have been determined from balloon meteorological data (Refs. 3 and 4).

An expression for  $\Delta\rho_{\text{model}}$  at an elevation angle  $E$  has the form

$$\Delta\rho_{\text{model}} = 10^{-6} \sum_1 N_{s_1} G(E, h_1) \quad (6)$$

Ref. 2. H. S. Hopfield, "Two-Quartic Tropospheric Refractivity Profile for Correcting Satellite Data," J. Geophys. Res., Vol. 74, No. 18, 20 August 1969, pp. 4487-4499.

Ref. 3. H. S. Hopfield, "Tropospheric Effect on Electromagnetically Measured Range: Prediction from Surface Weather Data," Radio Sci., Vol. 6, No. 3, March 1971, pp. 357-367.

Ref. 4. H. S. Hopfield, "Tropospheric Range Error Parameters: Further Studies," APL/JHU CP 015, June 1972 (also published as Goddard Space Flight Center Preprint X-551-72-285, August 1972).

where  $i$  takes the values 1 and 2 for the dry and wet components, respectively. The full expression for the function  $G(E, h_1)$  is given in Ref. 2. A simplified expression for easier computing is given in Ref. 5.

The following assumptions and approximations entered into the development of the model and the correction:

1. Ray-tracing methods can be used to determine the signal path; interference and diffraction phenomena are not considered. This assumption is retained here.
2. The temperature lapse rate in the un-ionized atmosphere is approximately  $6.8^\circ\text{C}/\text{km}$  and is constant. This is a good approximation for the troposphere proper but not for the stratosphere; however, the  $N_d$  model lumps them together. Since 80% of their joint effect occurs in the troposphere proper, below the tropopause (a still larger percentage at very low angles), the resulting mean error in using the  $N_d$  model may still be minor. Deviations from the mean may be significant, however, since temperature inversion layers and other irregularities actually are frequent but are disregarded in the model. Their effects will be seen in this study but only on a sample basis.
3. The  $N_w$  profile is written in the same quartic form as the  $N_d$  profile but does not have the same theoretical justification. Observed  $N_w$  profiles are very irregular.
4. Curvature of the signal path is neglected in deriving the correction based on the model. This effect is examined here.
5. Horizontal gradients of refractivity are still neglected in the present study; weather fronts are not considered.

The study is aimed toward improving the tropospheric correction for low-angle range and range-rate data. A little additional theory has been developed. Items 2, 3, and 4 in the above list of approximations have been studied with the help of some sample data. Various interesting findings are presented that have not yet been assimilated into a final, unified correction for low-angle data. This document is a progress report, not a final report on the subject.

---

Ref. 5. S. M. Yionoulis, "Algorithm to Compute Tropospheric Refraction Effects on Range Measurements," J. Geophys. Res., Vol. 75, No. 36, 20 December 1970, pp. 7636-7637.

## 2. THEORETICAL CONSIDERATIONS

### PROCEDURES FOR STUDYING LOW-ANGLE EFFECTS

#### Ray Tracing

The comparison of  $\Delta\rho_{\text{curve}}$  and  $\Delta\rho_{\text{st. line}}$  depends on knowing the path taken by a signal traveling through the atmosphere.

In collaboration with Harry K. Utterback, a computer program was developed for tracing the curving ray path of a signal at any elevation angle through an atmosphere with any specified refractivity profile (see Fig. 1). Details will be published in a document that is now being prepared. In brief, the program computes the geometrical length of the curved path and also its electromagnetic length ( $\int n ds$ ), using numerical integration. Both the geometrical and the electromagnetic path lengths are compared with the slant range vector ( $\rho$ ) having the same endpoints. The total bending angle is also determined. The program can use either a theoretical refractivity profile or one computed from observed meteorological balloon data (Ref. 3). Observed profiles are used here.

The heights at which meteorological data are measured by balloon instruments are considered as boundaries of successive atmospheric layers. The zenith angle ( $\beta_1$ ) of the ray at the surface of the earth is specified. The zenith angles ( $\beta_i$ ) at all the layer boundaries are then obtained from Snell's law for spherical surfaces:

$$n_i r_i \sin \beta_i = \text{constant} \quad (7)$$

where values of  $r_i$  are the radii of the layer boundaries from the center of the earth, and the constant is obtained from the known values at the surface. The ray path in each layer is assumed to be an arc of a circle. There are no discontinuities in the ray direction, but the radius of curvature changes at the layer boundaries. Each radius of curvature can be computed from the known zenith angles and layer heights. A mean value of  $n$  for each layer is used in the numerical evaluation of  $\int n ds$  along the curved path.

It should be noted that the boundary  $r_{\text{top}}$  (Fig. 1) represents the topmost height of the specific set of balloon observations, not the top of the atmosphere. Special methods developed to estimate the increments of range effect and signal path bending above  $r_{\text{top}}$  will be described in the forthcoming paper on the ray-tracing program.

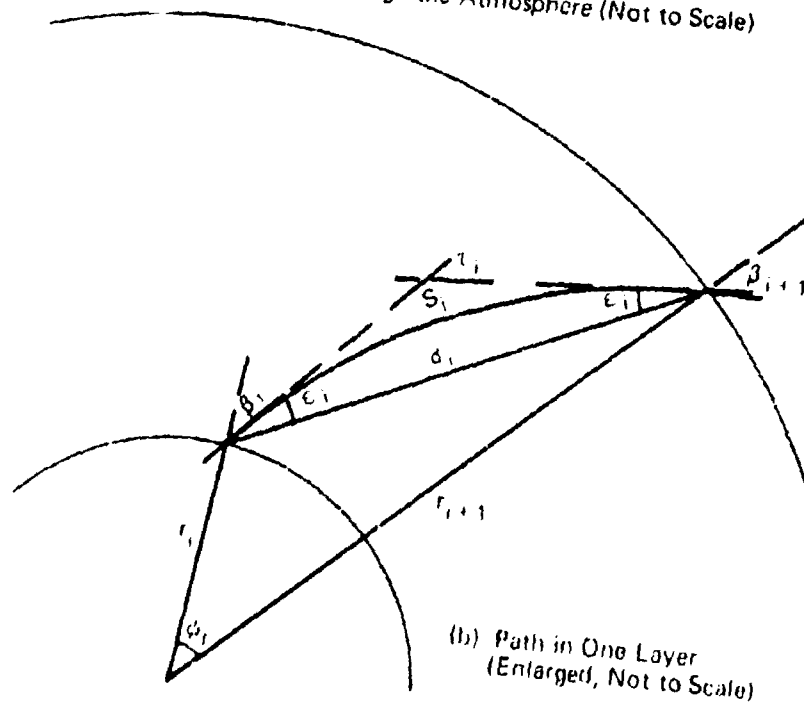
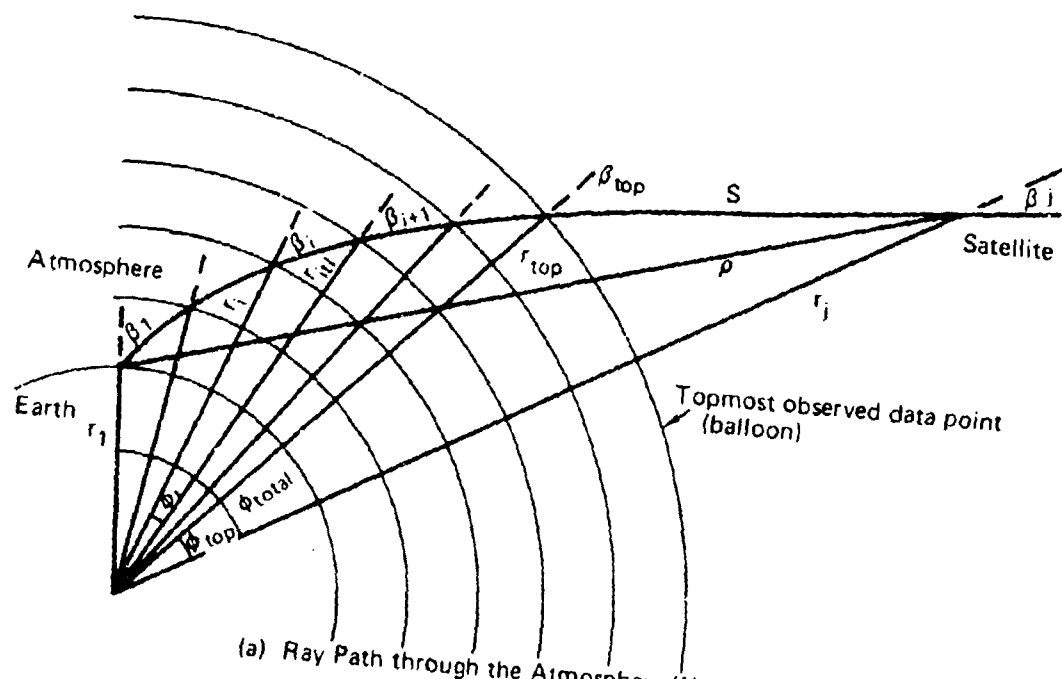


Fig. 1 Signal Path through the Atmosphere

The resulting value of  $\Delta\rho_{\text{curve}}$  for a particular atmosphere and elevation angle is our best estimate of the actual tropospheric range error under the specified conditions.

In addition, the refractivity is integrated along the slant range vector in two ways: (1) using the same refractivity profile as the ray trace to get  $\Delta\rho_{\text{st. line}}$ , and (2) using the two-quartic refractivity profile based on surface data only to get  $\Delta\rho_{\text{model}}$ .

#### Effect of Tropospheric Correction on Ground Station Position

A tropospheric correction based on the above theoretical refractivity profile is routinely applied to doppler data from navigational satellites. The effect of this correction on "navigating" a station position was studied for a few sample cases. The station position was determined with and without the use of the correction. The effect of changing the value of a height parameter of the model was also examined for a small sample of satellite passes.

#### SIGNAL PATH BENDING

For correcting range and doppler data, the angular bending of the signal path is of concern only insofar as it affects the electromagnetic path length. The actual signal path of length  $s$  is usually curved except in the zenith direction and is geometrically longer than the slant range, but it is electromagnetically shorter according to Fermat's principle (Ref. 6):

$$\begin{array}{l} s > \rho \\ \text{but} \\ \int_{\text{curve}}^{\text{nds}} < \int_{\text{st. line}}^{\text{nd}\rho} \end{array} \quad \left. \vphantom{\begin{array}{l} s > \rho \\ \text{but} \\ \int_{\text{curve}}^{\text{nds}} < \int_{\text{st. line}}^{\text{nd}\rho} \end{array}} \right\} \quad (8)$$

The ray-tracing results show that, to a good approximation,

$$\int_{\text{nds}} - \int_{\text{nd}\rho} \approx -(s - \rho) \quad (9)$$

The quantity  $(\int_{\text{nds}} - \int_{\text{nd}\rho})$ , the curvature error in the tropospheric correction, must be evaluated by ray-tracing techniques, but the quantity  $(s - \rho)$ , which is nearly equal to it in magnitude, can be studied geometrically for simple cases.

---

Ref. 6. G. Joos, Theoretical Physics, translated by Ira M. Freeman, Hafner Publishing Co., New York, 1934.

The bending effect on the signal path length is a few millimeters or less at elevation angles of 20° and greater, a few centimeters at 10° elevation, and a few meters at 1° elevation. The usefulness of low-angle data for geodetic purposes therefore depends partly on our ability to correct adequately for signal bending effects.

#### Amount of Bending

Path bending ( $\tau$ ) is produced by a refractive index gradient normal to the path, and the rate of bending ( $d\tau/ds$ ) along the path is proportional to this gradient. In a spherically layered atmosphere, the bending rate is (Ref. 7)

$$\frac{d\tau}{ds} = - \frac{\frac{dn}{dr} \sin \beta}{n} \quad (10)$$

where the definitions are the same as above. The negative sign is chosen to make  $\tau$  positive for a path that is concave downward, as in the real troposphere. Obviously there is no bending at the zenith, where  $\beta = 0$ . The total bending through the atmosphere is

$$\tau = \int \frac{d\tau}{ds} ds = \int \frac{d\tau}{ds} \frac{ds}{dr} dr \quad (11)$$

From geometry,

$$\frac{ds}{dr} = \frac{1}{\cos \beta} \quad (12)$$

Combining equations,

$$\tau = - \int \frac{1}{n} \frac{dn}{dr} \frac{\sin \beta}{\cos \beta} dr \quad (13)$$

$$= - \int \frac{\tan \beta}{n} dn \quad (14)$$

This equation is well known (Refs. 8 and 9) but is not easy to evaluate. It can be numerically integrated using a model of the

---

Ref. 7. J. E. Freehafer, "Geometrical Optics," Vol. 13, Chap. 2, Propagation of Short Radio Waves, D. E. Kerr (Ed.), M. I. T. Radiation Laboratory Series, McGraw-Hill Book Co., 1951, and Dover Publications, New York, 1965.

Ref. 8. W. M. Smart, Text-Book on Spherical Astronomy, Cambridge University Press, Cambridge, England, 1962.

Ref. 9. B. R. Bean and E. J. Dutton, "Radio Meteorology," National Bureau of Standards Monograph 92, 1 March 1966.

$n$  profile or data from an observed profile; or expansions and approximations may be used to get a general expression. Such approximations are generally valid at high elevation angles but not adequate at low angles.

A new approximate procedure is described below. It appears to be satisfactory down to a lower elevation angle than is ordinarily the case.

For this new procedure, we use

$$\sin \beta = \frac{n_1 r_1}{nr} \sin \beta_1 \quad (15)$$

from Snell's law (Eq. (7)); the subscript 1 now refers to values at the surface of the earth. Then

$$\cos \beta = \sqrt{1 - \left(\frac{n_1 r_1}{nr}\right)^2 \sin^2 \beta_1} \quad (16)$$

Dividing Eq. (15) by Eq. (16) and simplifying but making no approximations, we get

$$\tan \beta = \tan \beta_1 \frac{\frac{n_1 r_1}{nr}}{\sqrt{1 + \tan^2 \beta_1 \left[1 - \left(\frac{n_1 r_1}{nr}\right)^2\right]}} \quad (17)$$

Substituting Eq. (17) into Eq. (14) yields

$$r = -\tan \beta_1 \int \frac{\frac{n_1 r_1}{nr}}{\sqrt{1 + \tan^2 \beta_1 \left[1 - \left(\frac{n_1 r_1}{nr}\right)^2\right]}} \frac{dn}{n} \quad (18)$$

In the troposphere and stratosphere,  $n$  decreases as  $r$  increases. The product  $nr$  therefore changes more slowly than either factor separately. The ratio  $n_1 r_1 / nr$  changes by less than 1% up to 50 km above the earth and by less than 0.1% in the lowest 5 km of air, where half of the path bending occurs. It may be satisfactory to assume a constant value for this ratio, i.e., some reasonable mean value.

On this basis, let

$$R = \frac{n_1 r_1}{nr} = \text{constant} \quad (19)$$

and let

$$A(\beta_1) = \frac{R}{\sqrt{1 + \tan^2 \beta_1 (1 - R^2)}}, \quad (20)$$

which is no longer a function of  $r$ . Using these values, Eq. (18) becomes

$$\tau = -A(\beta_1) \tan \beta_1 \int_{n_1}^{1.0} \frac{dn}{n}. \quad (21)$$

This equation can be integrated to yield

$$\tau = A(\beta_1) \tan \beta_1 \ln n_1. \quad (22)$$

For  $2 > n_1 > 0$ ,

$$\ln n_1 = (n_1 - 1) - \frac{1}{2}(n_1 - 1)^2 + \frac{1}{3}(n_1 - 1)^3 - \dots$$

Since  $(n_1 - 1)$  is a very small quantity, only the first term need be used. Substituting a value from Eq. (3), we have for the total bending angle

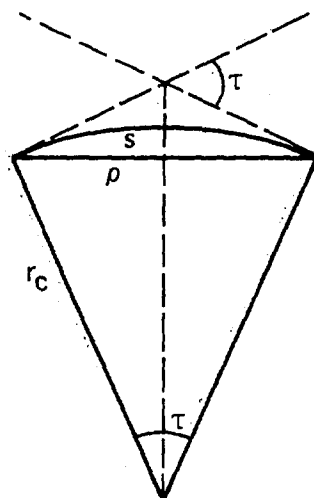
$$\tau = A(\beta_1) \tan \beta_1 N_1 \times 10^{-6} \text{ rad}. \quad (23)$$

This equation cannot be used when  $\beta_1 = 90^\circ$  (horizontally arriving ray). However, it does not imply an infinite value of  $\tau$ , since  $A(\beta_1) \rightarrow 0$  as  $\tan \beta_1 \rightarrow \infty$ .

Values of  $\tau$  computed from this equation will be compared in a later section with values obtained from ray tracing.

#### Range Effect of Bending

This effect is easily deduced for a hypothetical case where the path of the signal is an arc of a circle (see diagram).



The signal travels along a circular arc of length  $s$  to or from an object at a slant range  $\rho$  and is deflected through an angle  $\tau$ . The radius of curvature is  $r_c$ . From the geometry,

$$s = r_c \tau$$

$$\rho = 2r_c \sin \frac{\tau}{2}.$$

But

$$\sin \frac{\tau}{2} = \frac{\tau}{2} - \frac{(\tau/2)^3}{3!} + \frac{(\tau/2)^5}{5!} - \dots$$

Then

$$\rho = 2r_c \left( \frac{\tau}{2} - \frac{\tau^3}{48} + \frac{\tau^5}{3840} - \dots \right)$$

$$s - \rho = r_c \left( \frac{\tau^3}{24} - \frac{\tau^5}{1920} + \dots \right).$$

For small values of  $\tau$ , to first order,

$$s - \rho = \frac{r_c}{24} \tau^3. \quad (24)$$

In the atmosphere, short segments of the path may be approximated individually as circular arcs, but the path as a whole is not circular since the gradient of the refractive index is not constant (cf. Eq. (10)). No theoretical expression has been found to relate  $(s - \rho)$  to  $\tau$  for the real atmosphere, but an empirical relation will be illustrated in a later section.

### 3. NUMERICAL RESULTS

#### RAY TRACING

Figure 2 shows the magnitude of the tropospheric radio-range effect as a function of signal elevation angle at the surface of the earth. Any correction must try to match such effects. The values shown are means obtained from a one-month sample of meteorological balloon data. The ray-tracing procedure was used with the data of each balloon flight to determine  $\int n ds$  along the curving ray path at the time of the flight. The quantity  $(\int n ds - \rho)$  represents our best estimate of the tropospheric effect actually encountered by the signal. The slant range in each case is the range to the endpoint of that particular ray trace, 1000 km above the earth. The integral  $\int (n - 1) \rho d\rho$  computed along the slant range vector through the same atmosphere is the error estimate to the same endpoint when curvature of the signal path is neglected. Both sets of results are shown. The difference between the two is the error incurred by neglecting the bending. It is imperceptible at high angles but is significant at the horizon. The straight-line path gives the larger tropospheric effect (Fermat's principle).

Figure 3 shows the difference on a larger scale, for low elevation angles only. A radio-range correction that is perfect at the zenith but neglects the signal path bending is 3 cm too large at  $10^\circ$  elevation for this set of data, 19 cm too large at  $5^\circ$ , and 3 m too large at  $1^\circ$  (elevation angle of arrival; elevation of the corresponding slant range vector is  $0.4^\circ$ ). The values are means, with error bars at  $\pm \sigma$  for the lowest angles. Radio effects in summer would be a little larger; effects on optical data (i.e., laser) would be slightly smaller than those in Fig. 3.

Results from the ray-tracing procedure provide interesting sidelights on the problem. Some of these will be included among the following figures.

Figure 4 shows the cumulative bending effect on a radio signal going out from the earth, as a function of height in the atmosphere, for two sample atmospheres, a summer and a winter sample. Most of the bending occurs in the lower part of the atmosphere. The greater radio signal bending by the summer atmosphere is a result of the greater water-vapor content. Irregularities in the atmosphere have a visible effect, but it is not conspicuous in this small-scale figure. The irregularities are emphasized in Fig. 5.

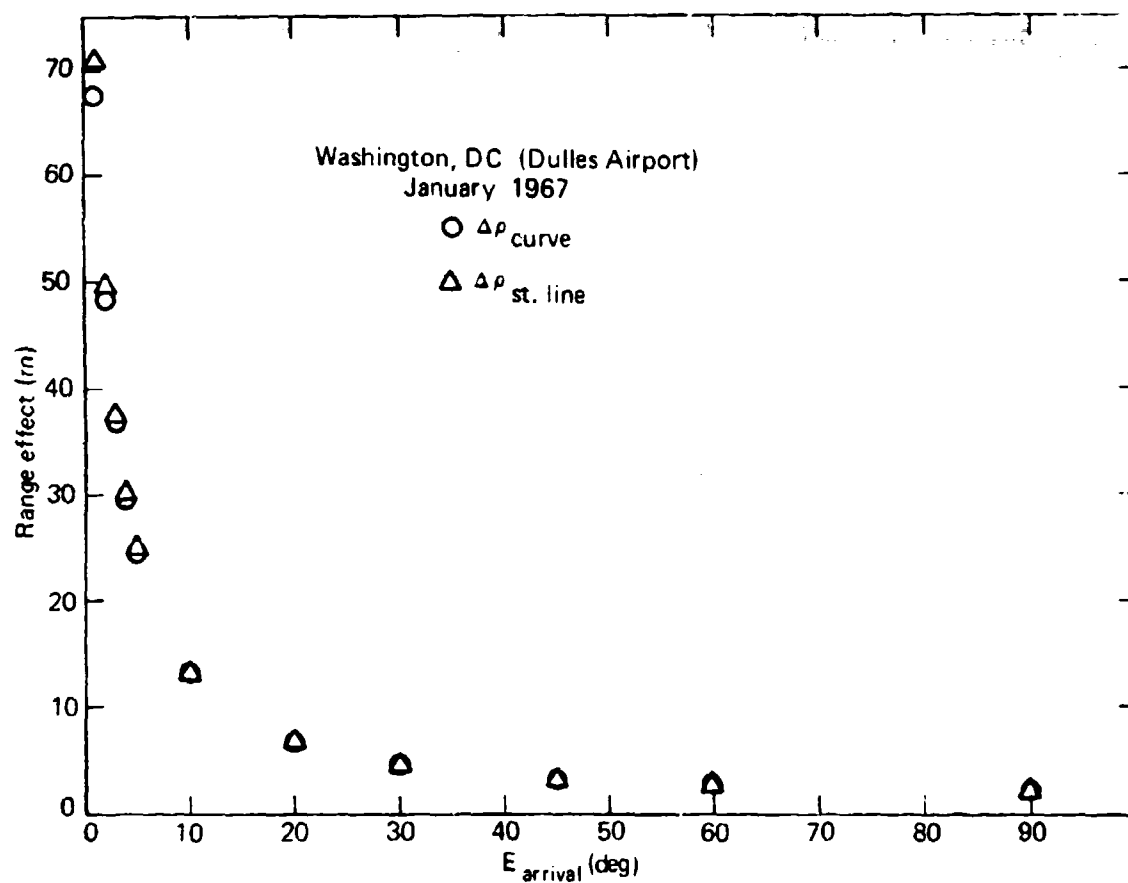


Fig. 2 Mean Tropospheric Range Effect on a Radio Measurement at Oblique Angles

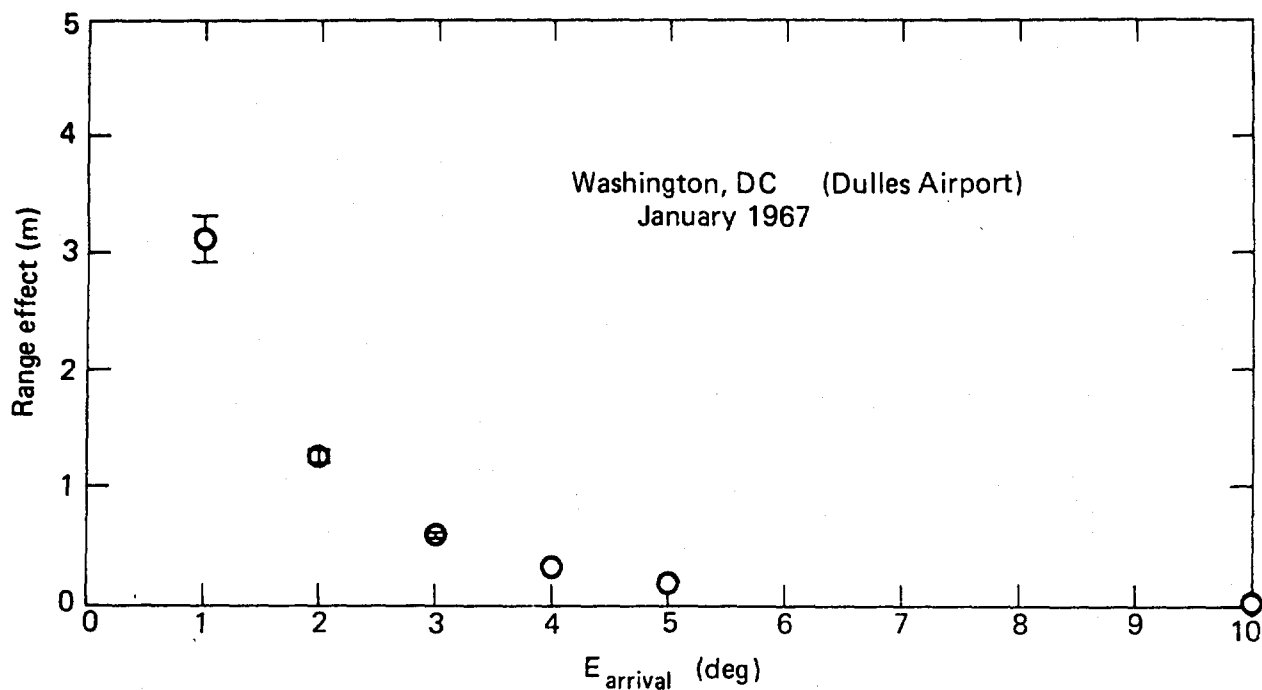


Fig. 3 Effect of Signal Path Bending on Radio Range Measurement,  $\Delta\rho_{\text{st. line}} - \Delta\rho_{\text{curve}}$

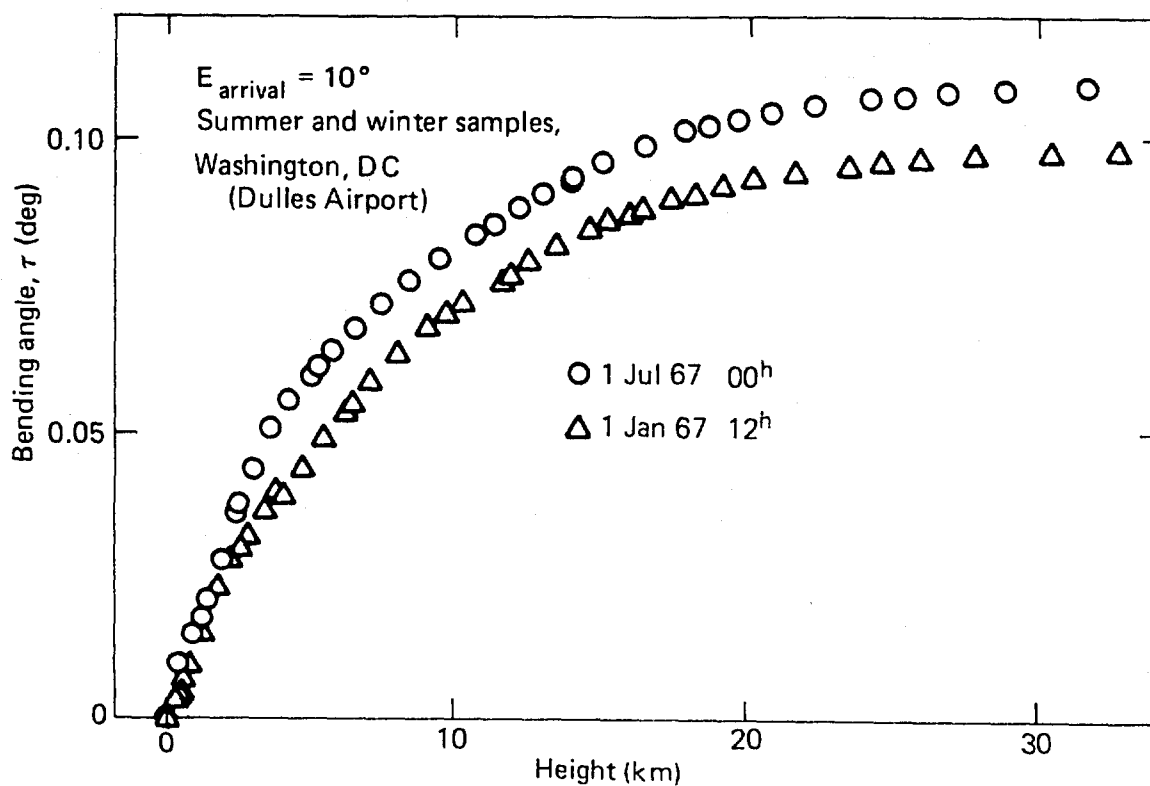


Fig. 4 Cumulative Angular Bending of Radio Signal Path versus Height above the Earth

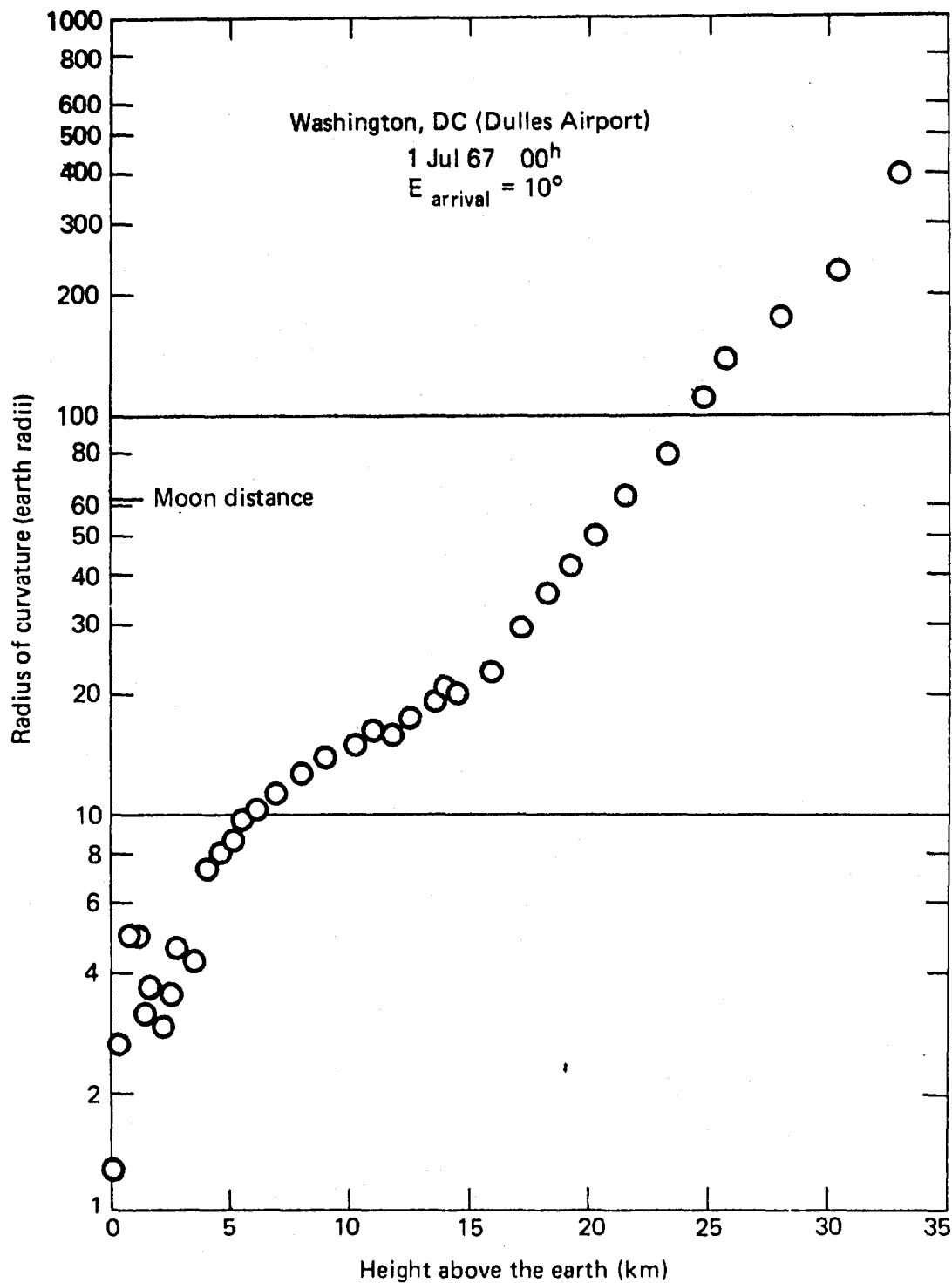


Fig. 5 Radius of Curvature of Radio Signal Path versus Height above the Earth

Figure 5 shows the radius of curvature of the signal path, layer by layer of the atmosphere, for one of the ray traces of Fig. 4, also at an elevation angle of  $10^\circ$ . The effect of irregular water-vapor and temperature profiles in the lower atmosphere is very conspicuous. Above the water-vapor region, the radius of curvature increases along a smooth but not a simple curve and shows the effect of the change of temperature regime at the tropopause. In one thin layer near the earth, the radius of curvature of the signal was little greater than the radius of the earth; at a height of 22 km above the earth, it was as great as the earth-moon distance.

Figure 6 shows the same bending angles as in Fig. 4, but as a function of the refractivity along the path (here plotted so as to decrease to the right on the graph, i.e., upward). The cumulative angular bending for a ray at a given elevation angle is nearly a linear function of refractivity. This is in agreement with the theory discussed above. The two atmospheric samples yield parallel lines so that the larger total bending results from the larger surface value of  $N$  (cf. Eq. (23)). This statement is illustrated by the next figure.

Figure 7 shows the total angular bending for winter and summer samples, but for a lower angle than in Fig. 6, plotted against  $N_{\text{surface}}$ . Both optical ( $N_{\text{dry}}$  alone) and radio (total  $N$ ) effects are included in the figure, with the bending angle obtained from ray tracing. The data separate themselves into natural groups, but all lie along a nearly straight line, as predicted by Eq. (23). Optical signals (dry component) are bent less in summer than in winter (lower air density gradient), but radio signals are bent more in summer than in winter (more water vapor). However, the slope of the empirical line is a little too steep for the line to go through the origin. The derivation of Eq. (23) included some approximations, which must be studied further.

For correcting range data, it is not actually the bending angle that is needed but the effect of the signal path curvature on measured range. Figure 8, obtained from ray tracing, shows this effect for signals arriving at the same low elevation angle ( $3^\circ$ ) under various weather conditions. The data sample includes data for the first half of January and July, respectively (same sample as in Fig. 7). The effect of bending on measured range is plotted against surface refractivity. There is a fairly linear relation but with considerable scatter, doubtless due to refractivity profile irregularities. Figures 7 and 8 show obvious correlation, but  $N_{\text{surface}}$  is a better predictor of the bending angle than of its range effect. It is possible that  $P_{\text{surface}}$  may be a better predictor of these effects than  $N_{\text{surface}}$  for the dry component alone.

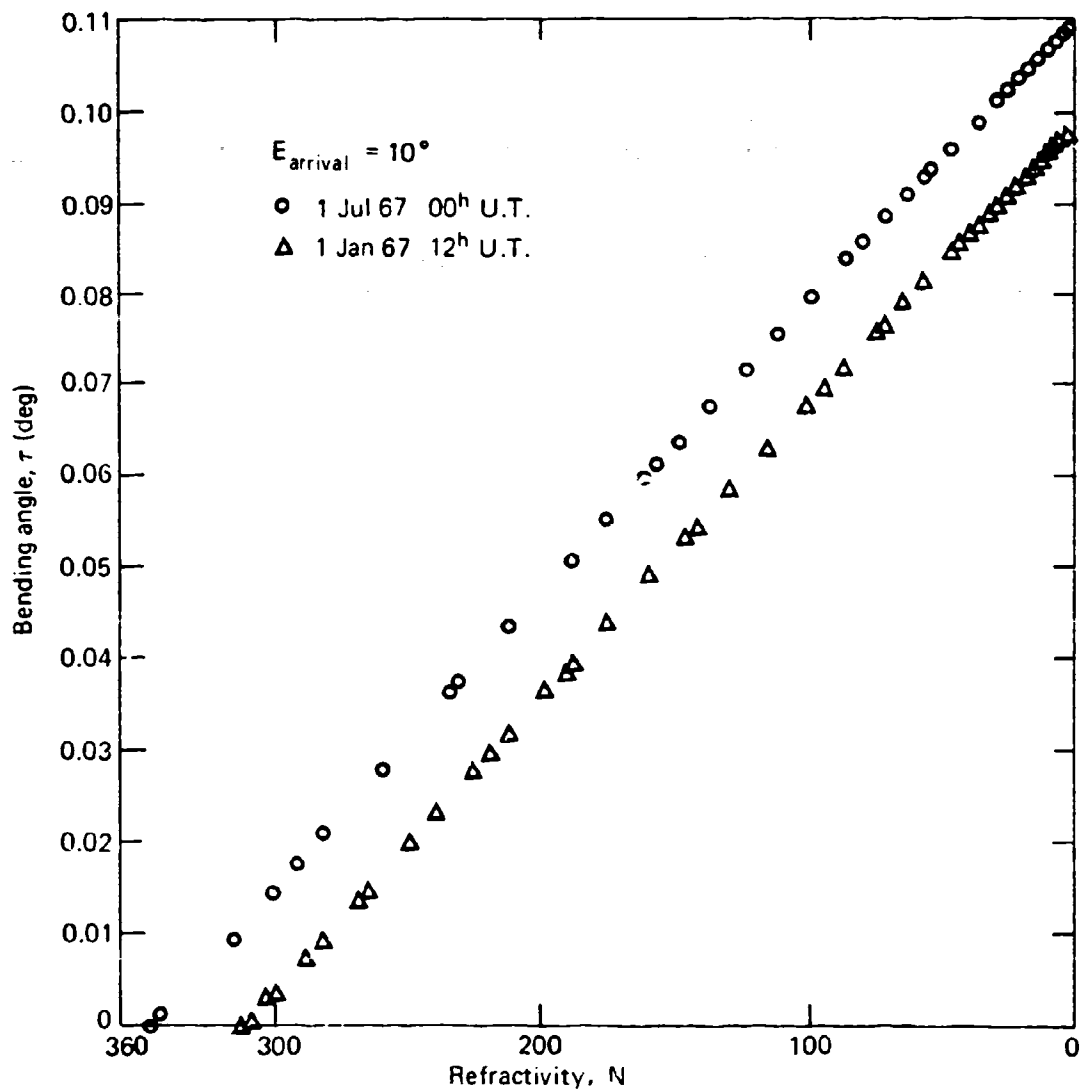


Fig. 6 Cumulative Angular Bending of Radio Signal Path versus Refractivity along the Path

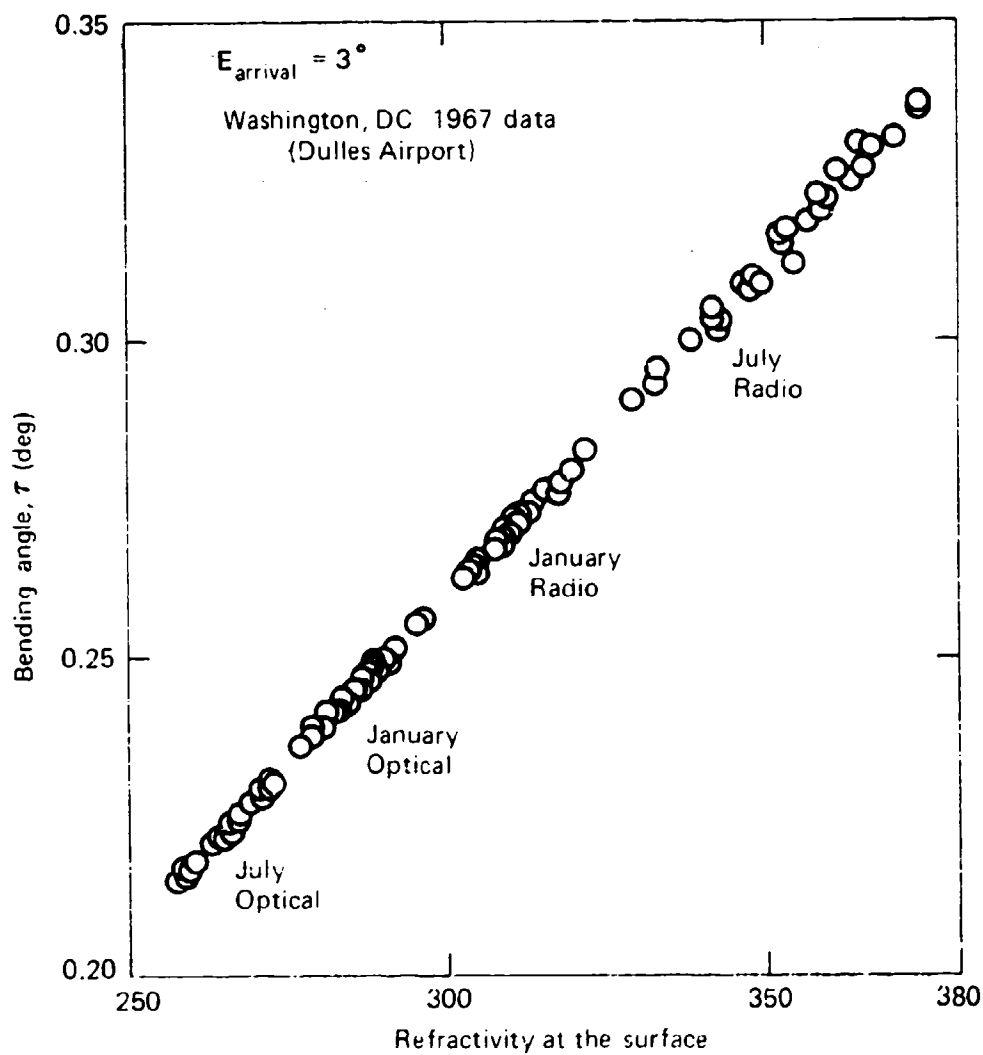


Fig. 7 Total Angular Bending of Signal Path versus Surface Refractivity

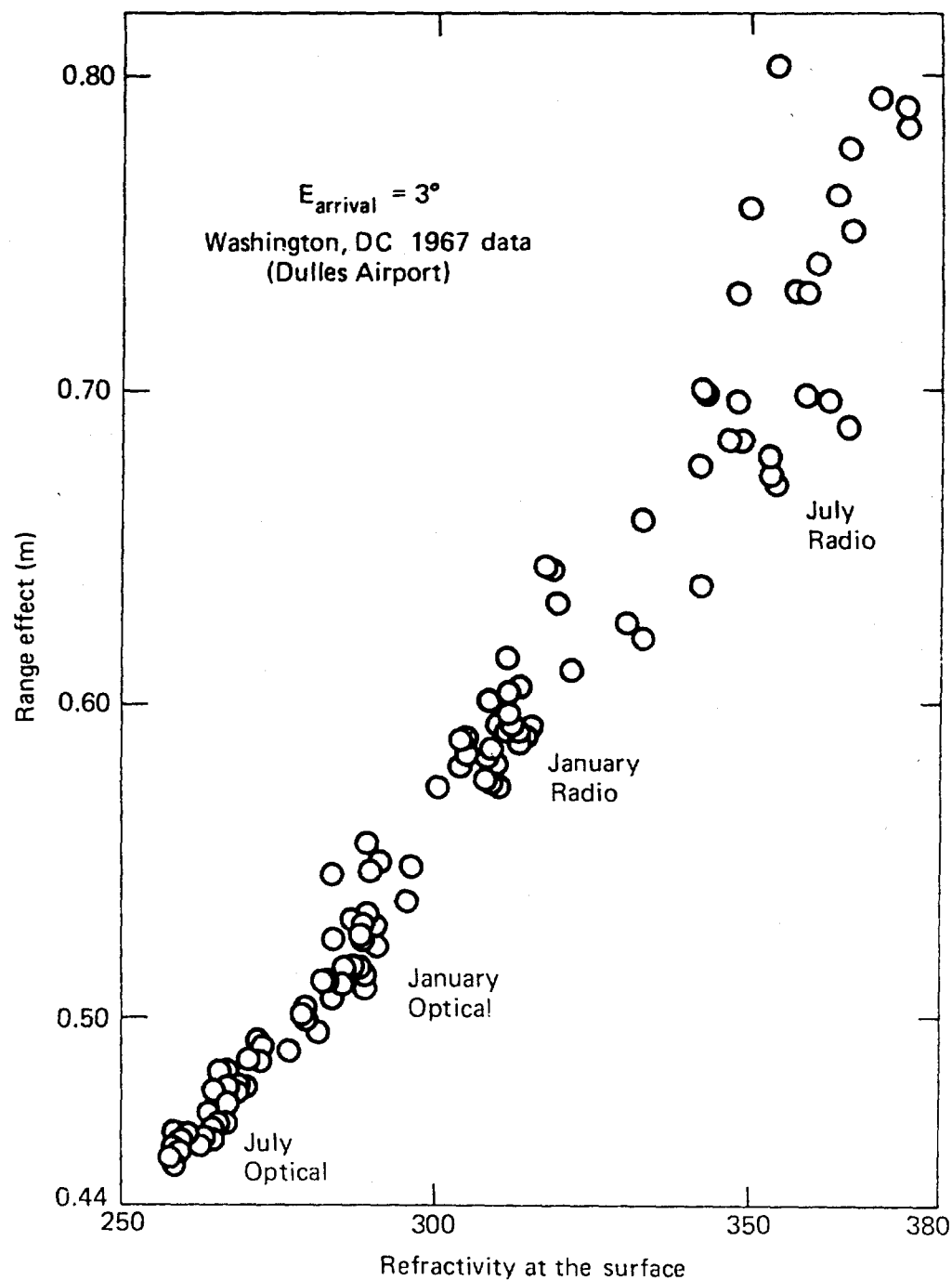


Fig. 8 Range Effect of Signal Path Bending versus Surface Refractivity

(as it is for high-angle effects), but this is not likely to be true for the radio case. The matter is being studied further.

Equation (23) provides a means of predicting the bending angle from surface data at any angle, if a value is postulated for the ratio ( $R$ ) of Eqs. (19) and (20). Figures 9 and 10 (optical and radio, respectively), show this predicted bending as a function of elevation angle ( $E \equiv (\pi/2) - \theta$ ) for an observed atmosphere, and also the bending determined by ray tracing through the same atmosphere. Three different values of  $R$  are used for theoretical prediction in each case. The differences among them are insignificant at high elevation angles but can be seen below  $10^\circ$ . In each case, the ray-traced values of  $\tau$  follow one of the theoretical predictions down to approximately  $3^\circ$  elevation and depart from theory below that. However, different values of  $R$  are needed in the optical case than in the radio case. The larger value that is needed in the radio case implies a lower "center of gravity" for the radio bending effect than for the optical bending effect; this would be expected because of the water-vapor distribution.

It may be possible to develop an empirical weighting function for  $R$  so as to make a prediction valid at still lower angles. Climatic and weather effects on the best value of  $R$  also need to be investigated.

We have no theoretical expression for the effect of path curvature on range error estimation in the real atmosphere as a function of bending angle. Figure 11 shows the effect computed by ray tracing. If the entire path were an arc of a single circle, the curvature effect on range would vary as  $\tau^3$ , but this is not the case. Figure 11 shows the path curvature effect as a function of  $\tau$  for one observed atmosphere. The observed line on the log-log paper is almost straight and its slope indicates that the curvature effect in that atmosphere was proportional to  $\tau^K$  where  $2 < K < 3$  and  $K$  probably has a value not far from 2.5. No statistical study of this relation has been made as yet. Further work is planned.

#### MODEL PREDICTIONS AT LOW ANGLES

In developing an oblique-angle correction from the troposphere model, it was assumed that bending of the signal can be neglected. Range effects obtained from the model should therefore be compared to values obtained by numerical integration along a straight line, as in the preceding section. If they can be made to match at low as well as at high angles, it will still be necessary to apply a curvature correction.

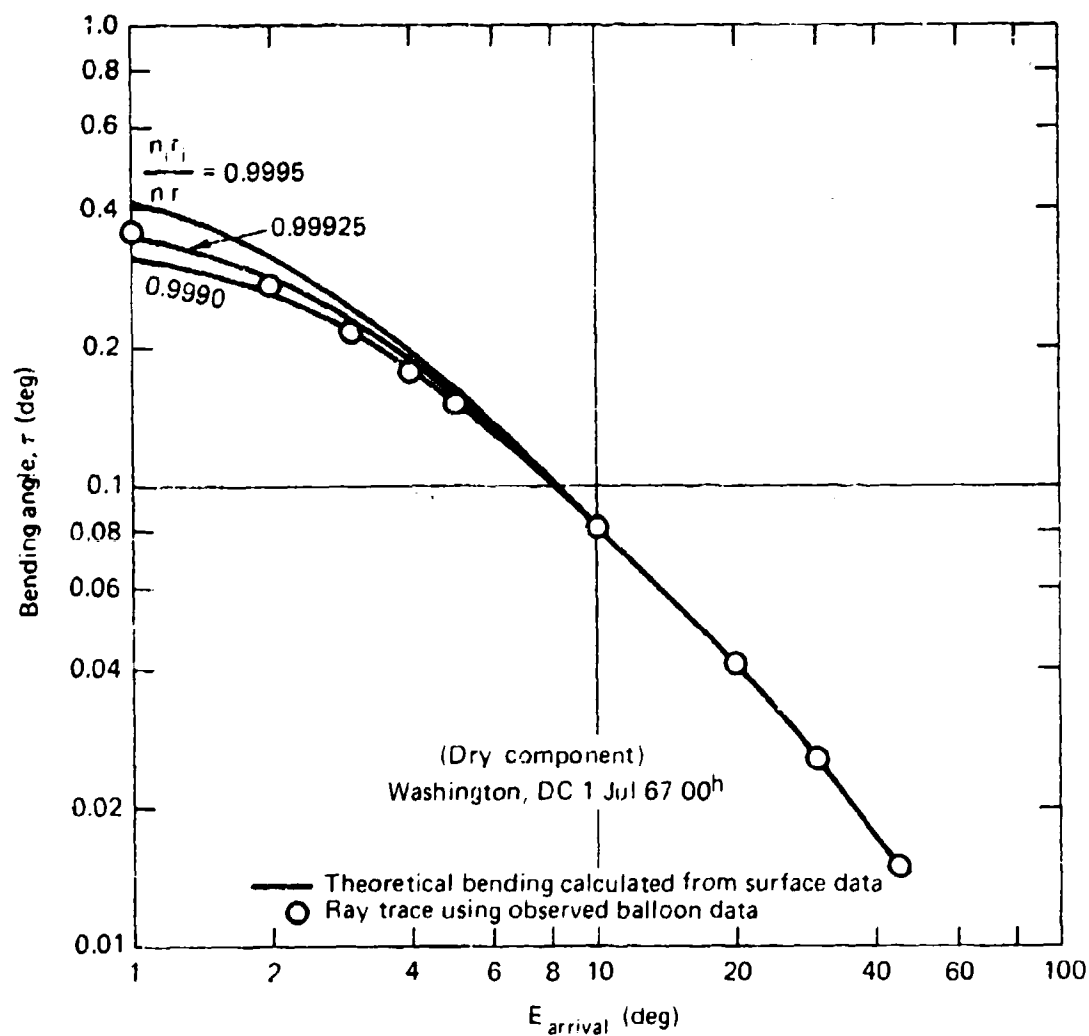


Fig. 9 Optical Signal Path Bending, Theoretical and Ray Traced

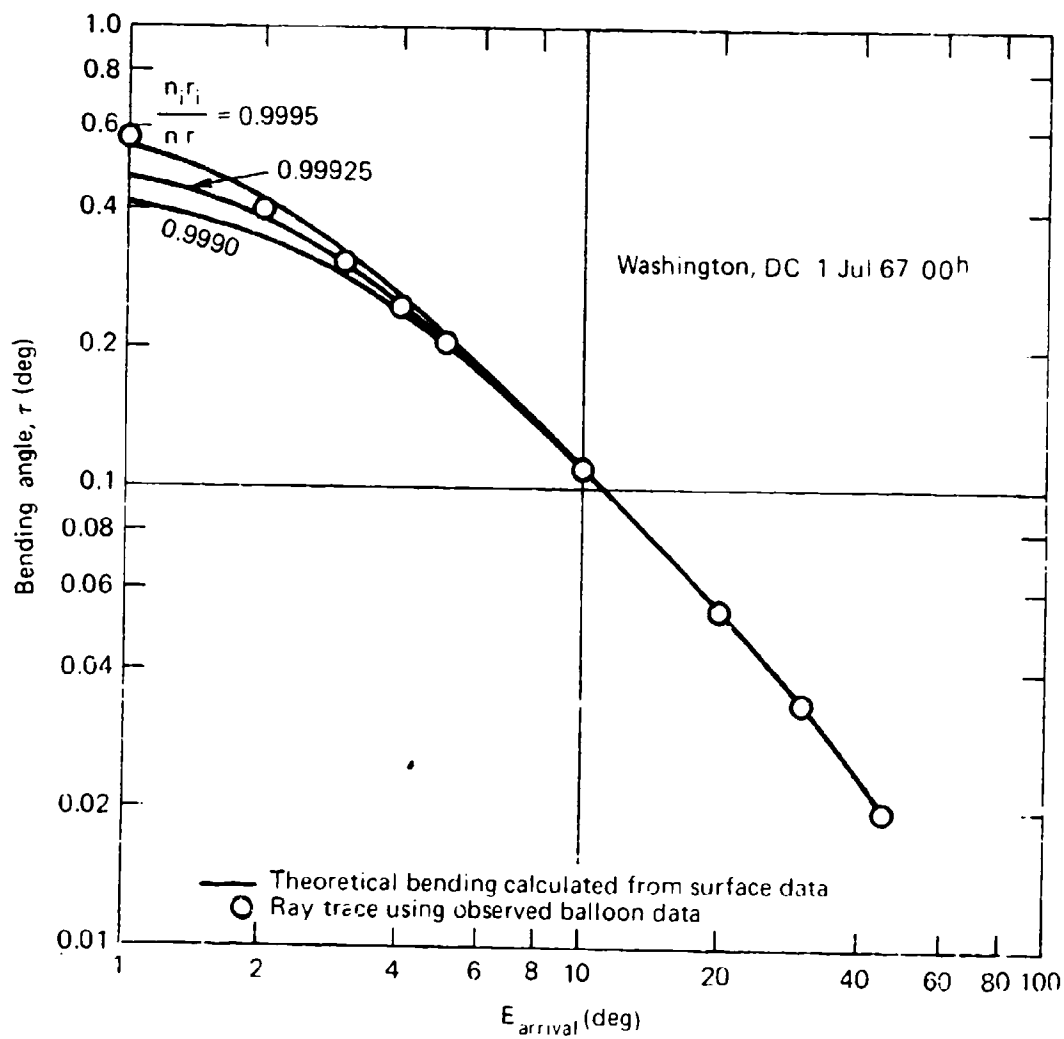


Fig. 10 Radio Signal Path Bending, Theoretical and Ray Traced

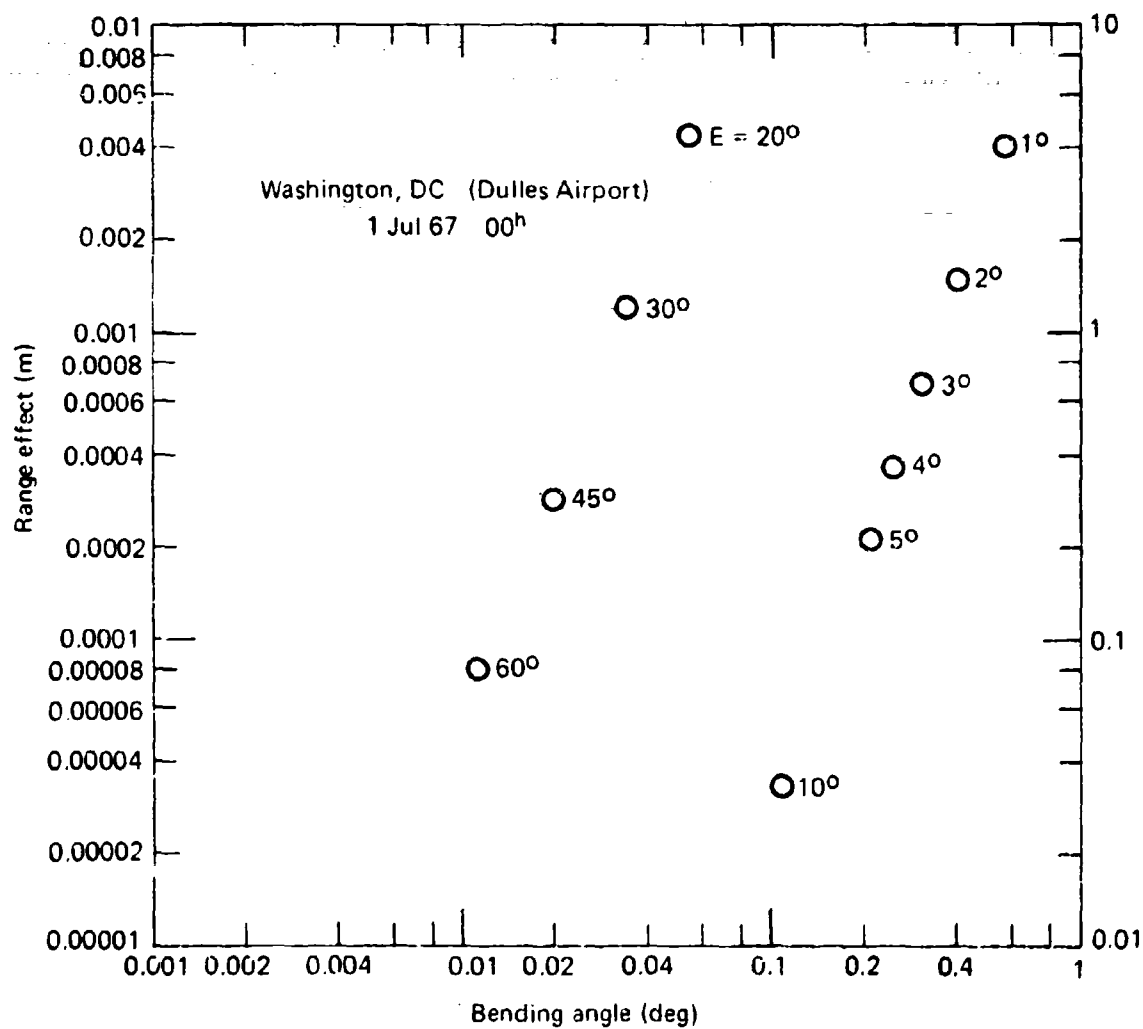


Fig. 11 Effect of Path Bending on Radio Range, versus Bending Angle

The possibility should also be considered that the model or its parameters could be adjusted to match results computed along the curved path at low and at high angles. In this case, no separate curvature correction would be needed, a result that is preferable but less likely to be achieved. We first must learn how actual model predictions compare with straight-line and curved-path numerical integration results.

Figures 12 and 13 show the difference between predictions from the model using surface data and numerical integration along a straight-line path using balloon data. The figures show a winter and a summer sample. Two values of the water-vapor height parameter for the model are used for each month.

The discrepancy between the model and the observed atmosphere varies with elevation angle. For most cases, it increases toward the horizon. It is possible to match the two effects perfectly at the zenith for any reasonable model profile by choice of parameters, but only a perfect match of refractivity profiles (model versus observed) would match effects perfectly at lower angles also. Work will continue on improving the matching.

The lower-angle error that is introduced by the present model is sensitive to the choice of height parameters, as can be seen in the figures. The parameter for dry-component height, in the latest form of the model (used in these figures), is a linear function of surface temperature. No weather adjustment is now used for the wet-component height, but low-angle data may provide criteria for making such an improvement. Further work along this line is planned.

Comparison of Figs. 12 and 13 with Fig. 3 shows that signal path bending is a larger contributor to prediction error at low angles than is model inaccuracy. The total prediction error includes both of these. At some angles and with some parameter values the two range effects may have opposite signs, so that a tradeoff might be possible. Figures 14 and 15 show winter and summer samples, respectively, of the difference between the model prediction and the actual tropospheric effect computed along the curving signal path. The values shown are one-month means, and error bars show the standard deviation from the mean. These are the prediction errors that should be expected after the present model correction is made. The mean errors for winter and summer are not too different, but the scatter is much worse in summer because of the large and variable water-vapor content.

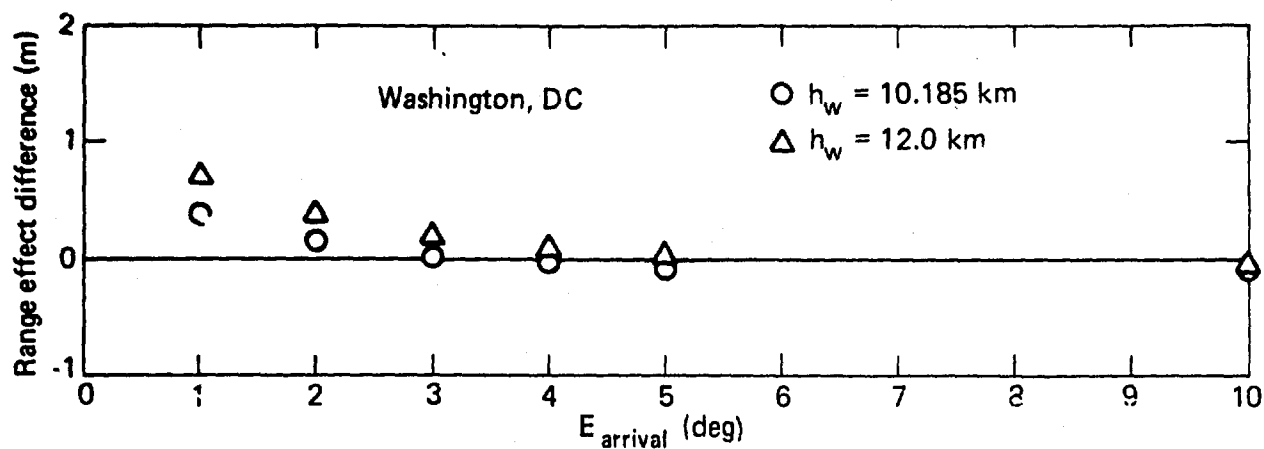


Fig. 12 Range Effect Difference for Radio Signal,  $\Delta\rho_{\text{model}} - \Delta\rho_{\text{st. line}}$ , January 1967

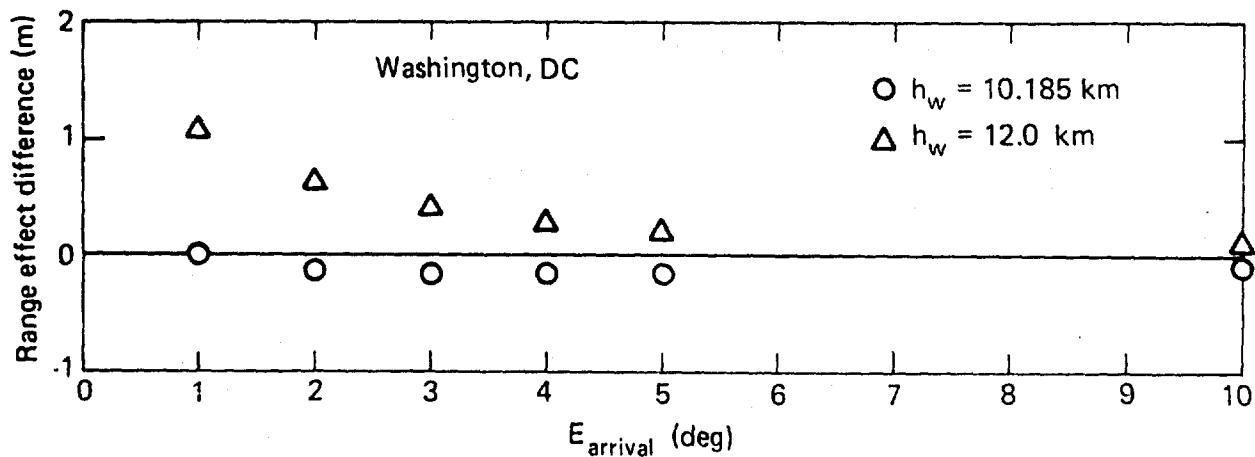


Fig. 13 Range Effect Difference for Radio Signal,  $\Delta\rho_{\text{model}} - \Delta\rho_{\text{st. line}}$ , July 1967

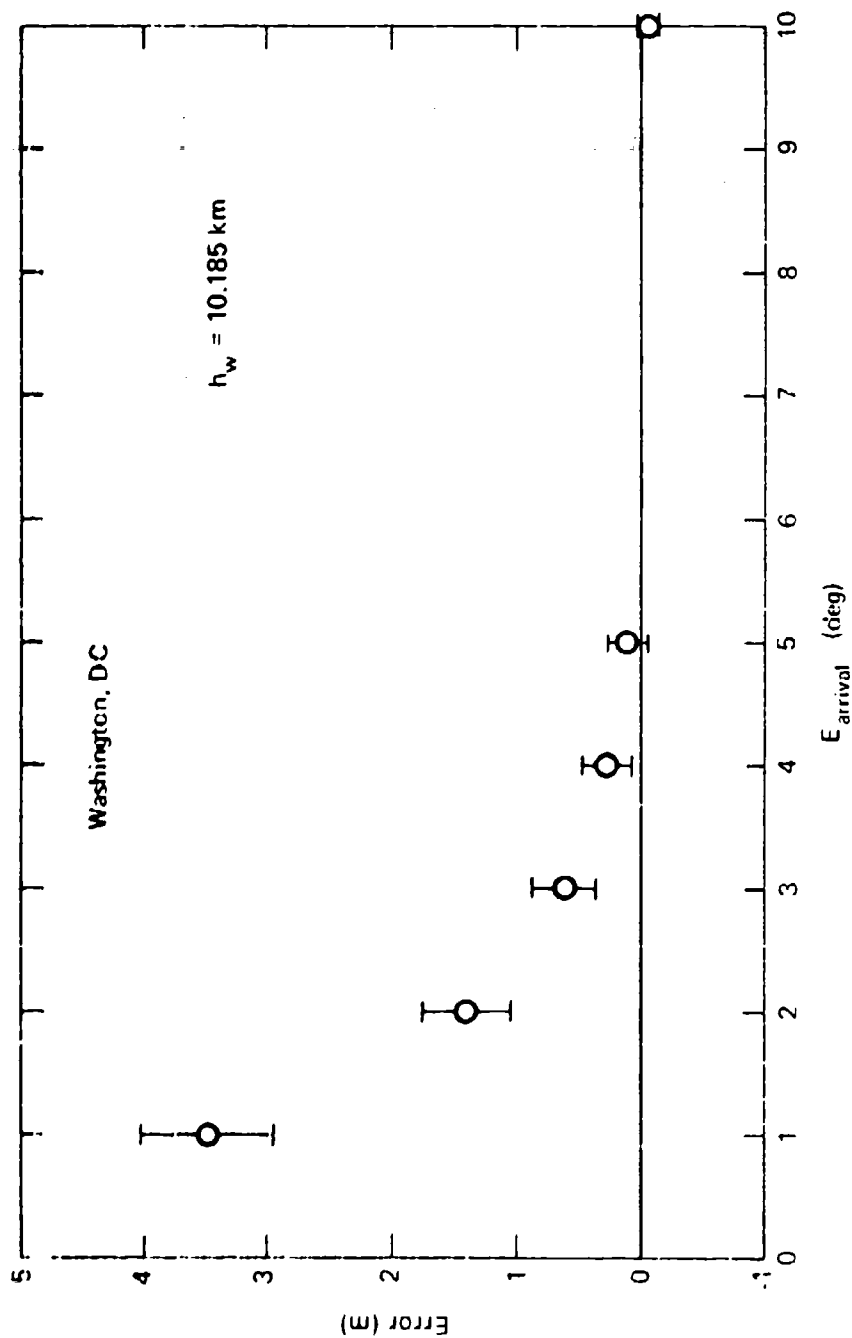


Fig. 14 Total Error in Model Estimate of Tropospheric Effect,  $\Delta \rho$  model  $-\Delta \rho$  curve for Radio Signal, January 1967

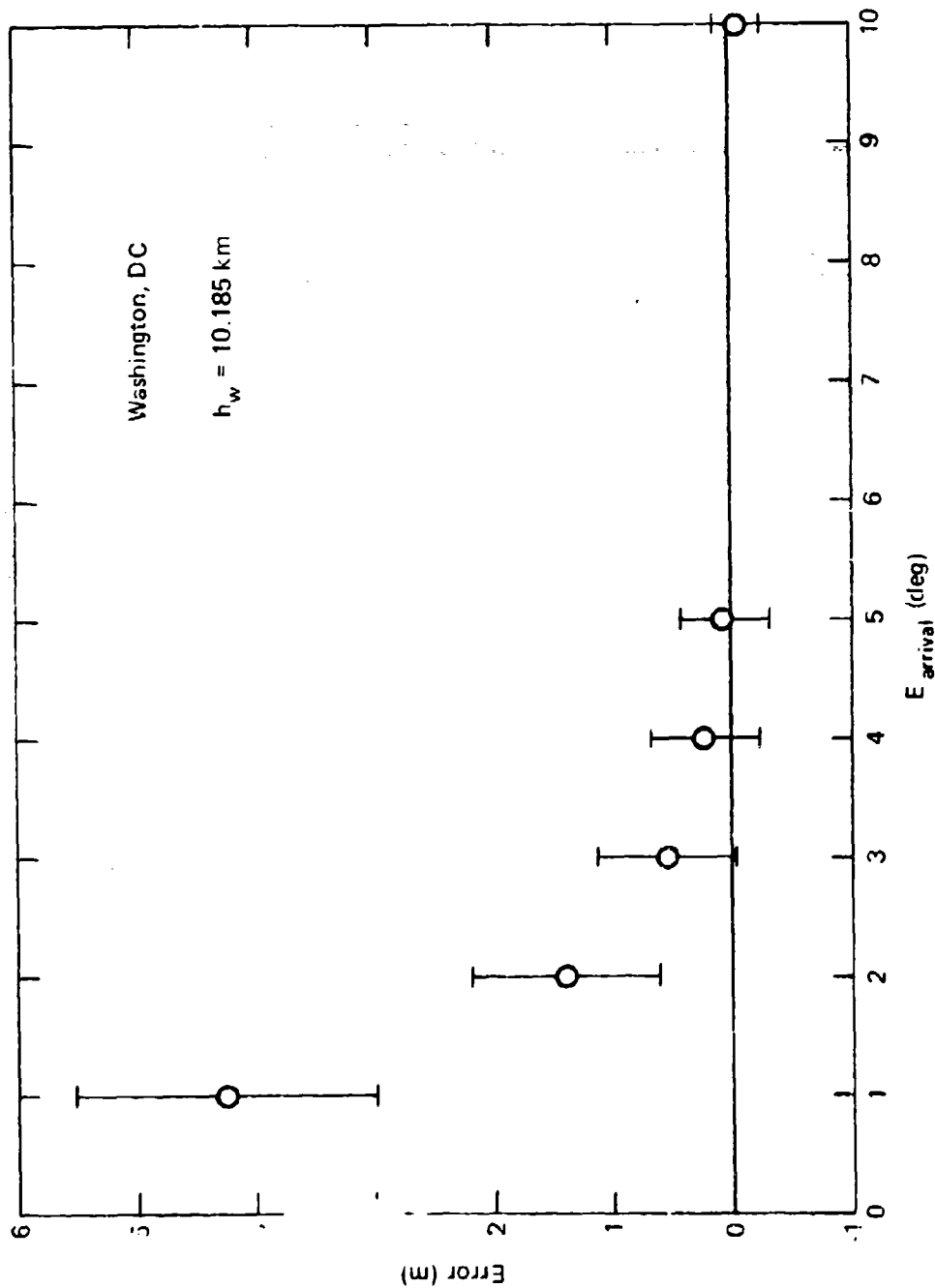


Fig. 15 Total Error in Model Estimate of Tropospheric Effect,  $\Delta \rho_{\text{model}} - \Delta \rho_{\text{curve}}$  for Radio Signal, July 1967

## EFFECT OF TROPOSPHERIC CORRECTION ON STATION POSITION

When satellite doppler data are used to determine the position of a tracking station, the uncorrected tropospheric effect introduces an error into the computed station position. The apparent range to the satellite is too great at every point of the pass, but this error is very much greater at the horizon than at the point of closest approach. The time derivative of the observed doppler shift is therefore too great, and the station appears to be closer to the orbit than it really is. The effect is greater for low-angle than for high-angle satellite passes. Only the apparent range is affected if tracking data are symmetrical about the point of closest approach; if not, the apparent station position may also be shifted parallel to the orbit.

Figure 16 shows the range effect only. The range error, with no tropospheric correction, determined for each of a set of passes at the Maine OPNET station is plotted as a function of elevation angle of the satellite at closest approach. Each point represents a satellite pass. The entire computation was then repeated with the tropospheric correction included. Both sets of results are shown in Fig. 16. No weather data were recorded, and statistical values were used as a basis for the computed correction.

Range errors without tropospheric correction varied from approximately 12 m for high-angle passes to 55 m for some lower-angle passes. Use of the correction left little range error in the high-angle passes, but the low passes were apparently over-corrected. This might be related to height parameters (cf. Figs. 12 and 13), to the neglected bending effect (Fig. 3), or to the use of statistical weather data instead of observed.

Figure 17 shows the same kind of data but for a different location, the Hawaii OPNET station. Again, the high-angle passes were corrected adequately. The correction for the lowest pass, however, was too small, in contrast to Fig. 16. Again, there is a question about height parameters and surface weather data.

Figures 16 and 17 include data down to an elevation angle of  $1^\circ$  when available. The navigation procedure was repeated with a data cutoff angle of  $5^\circ$ , with no appreciable change in the results. The reason is not certain, but it is possible that most of the passes were actually not tracked much lower than  $5^\circ$ . It would be desirable to continue this study in more detail.

The lack of surface meteorological data for the computations that produced Figs. 16 and 17 means that the correction was

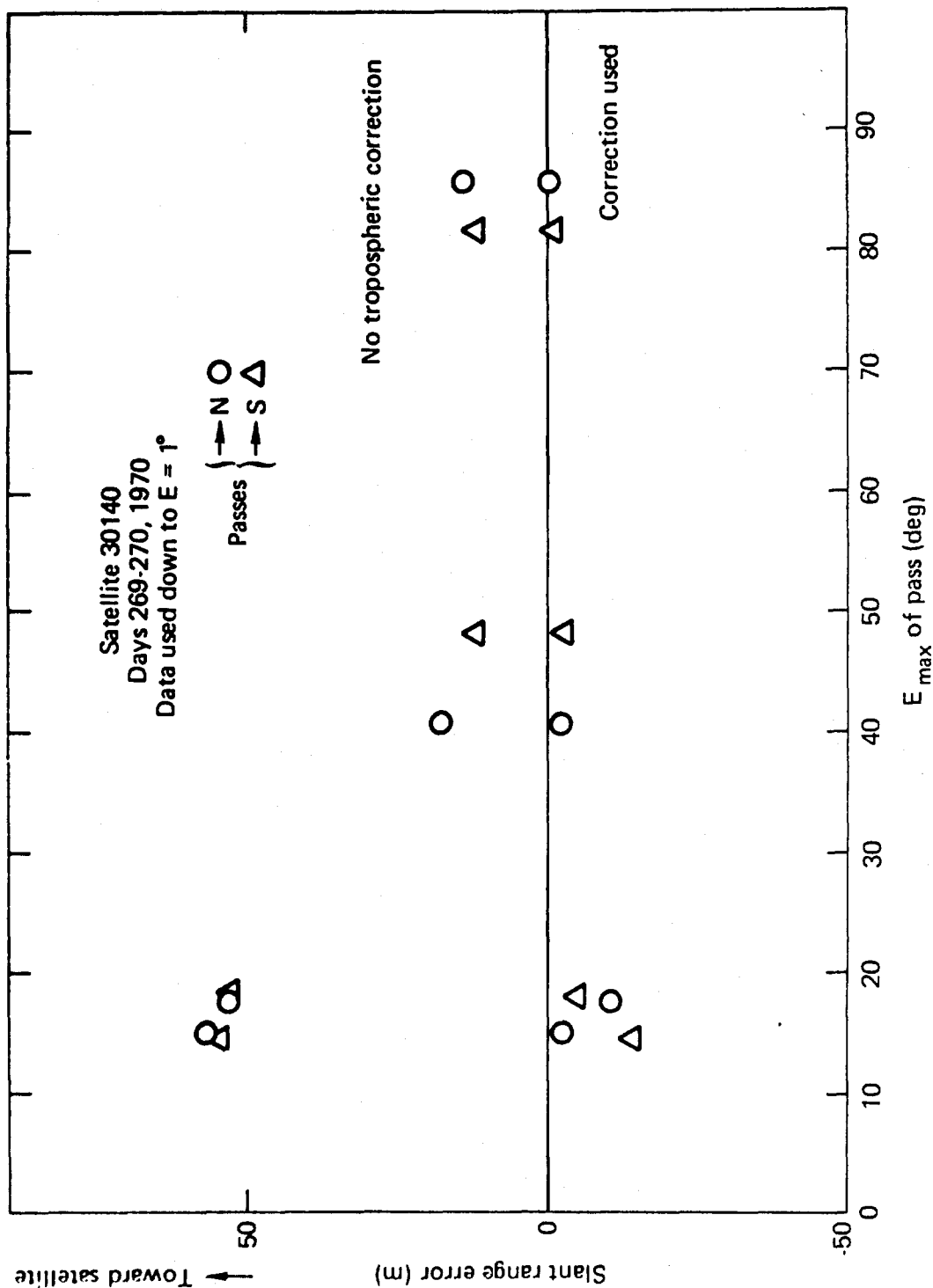


Fig. 16 Effect of Tropospheric Refraction on Apparent Tracking Station Position,  
Winter Harbor, Maine

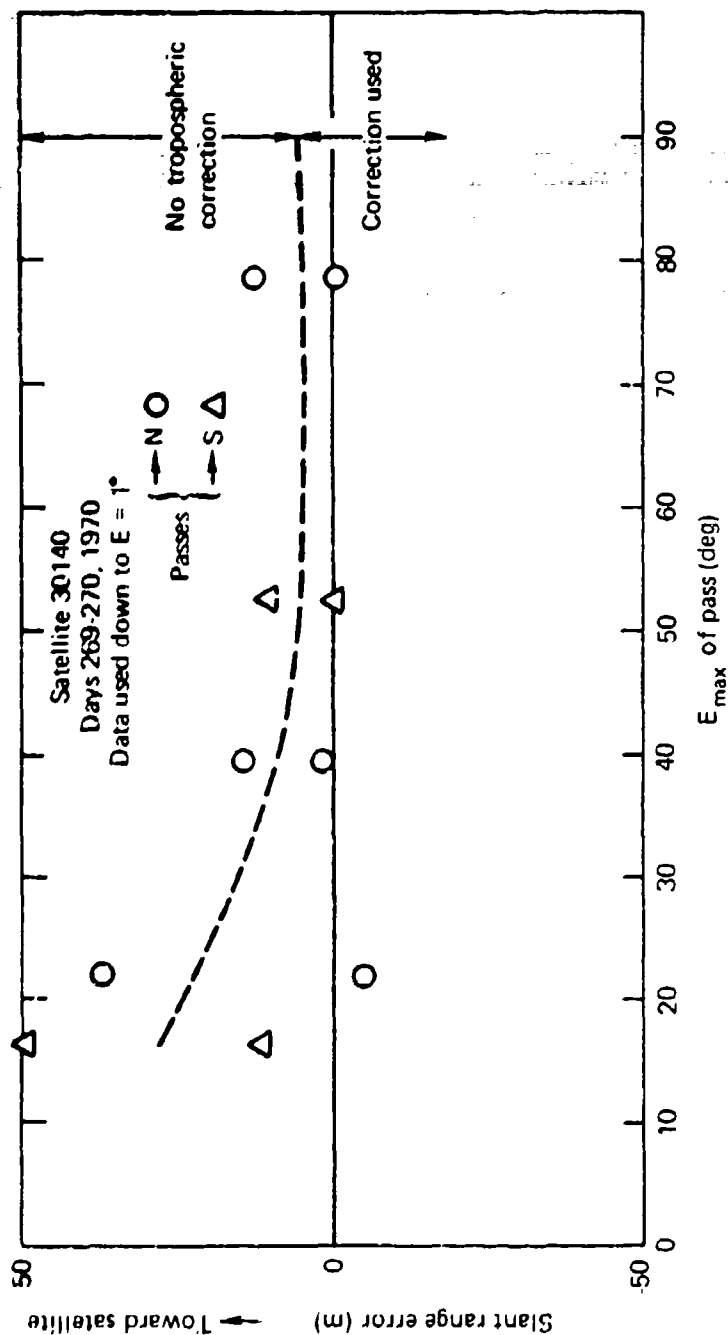


Fig. 17 Effect of Tropospheric Refraction on Apparent Tracking Station Position, Wahiawa, Hawaii

based on seasonal values of the refractivity, not on actual values at the time. This lack also precludes the use of the latest formulation for  $h_q$  (Refs. 3 and 4). The use of observed surface data could not be expected to change the navigation results by more than a few meters, even for low passes. However, the importance of a few meters has increased in recent years.

The positions of Figs. 16 and 17 were recalculated using a larger value for  $h_w$  than before, 12 km instead of 10 km. The corrections were a little larger than before, as expected, and shifted apparent station positions in the slant range coordinate by a few centimeters for the very high passes and about 1 m for the low passes. Changes in the dry component would have more effect, but no further experimentation has been carried out.

#### 4. SUMMARY OF PRESENT STATUS AND FUTURE PLANS

The purpose of this effort is to make possible the use of satellite range and/or range-rate data for precise studies at lower angles than are now practicable. To this end, the tropospheric refraction correction must be as accurate as possible.

A correction that was based on high-elevation-angle considerations was the result of earlier studies (Refs. 2 through 5). Although that correction can be used at any angle, its accuracy deteriorates, by a moderate percent, toward the horizon. This report describes the progress made to date in learning more about the low-angle effects and how to include them in an improved tropospheric correction. Bending of the signal path, neglected earlier, is now taken into account. Also, adjustment of the mathematically modeled correction for better correspondence with the real atmosphere is under study.

Plans for further study may be summarized under the following broad categories. Some of the items have been mentioned in the preceding discussion.

##### UPDATING OF THE DATA BASE

Most of the meteorological data on hand are for the year 1967, the most recent data available when the detailed study of balloon data was begun. Only small amounts of older and newer data have been obtained. Balloon data-gathering techniques have improved in the intervening years. In particular, there are now better instruments for measuring relative humidity. Although the water-vapor component accounts for only a small fraction of atmospheric refractivity, it is important because it is responsible for most of the variation and the difficulty in estimating the effect from surface data. Study of more recent balloon data is indicated.

There is a further possibility of a side benefit here. Extension of the data base in time might also provide hints, at least, of a solar-cycle effect on the atmosphere. (It is also of interest that the cost of obtaining balloon data from the National Climatic Center has decreased because of improved procedures at the Center.)

#### MORE RAY-TRACING STUDIES

The present troposphere model should be compared with additional observed data covering different geographical locations. The effects of varying the model parameters should be further investigated. The present parameters are designed for high elevation angles. A method should be sought for adjusting the model to fit propagation at all angles, low as well as high. Possibly a multiplicative correction factor can be found, e.g., a function of the elevation angle ( $F(E)$ ), a "correction for the correction."

This factor might provide the correction for agreement with hypothetical straight-line propagation through an observed atmosphere (in which case, a correction for the curvature effect must be provided separately), or it might include the curvature effect. The choice itself is a matter for study. Either case calls for more study of the bending effect with regard to climatic and weather variations.

#### MORE NAVIGATION STUDIES

Navigation results should be examined for a larger sample of stations and satellite passes. Preferably, locally observed surface weather data should be provided with the tracking data and used with the model. The effects of varying the model parameters and of changing the data cutoff angle should be studied and compared with expectations based on ray-tracing results.

If a new correction factor ( $F(E)$ ) for improving the tropospheric correction is developed by ray-tracing techniques, the final evaluation should make use of satellite data.

Even if local balloon data were available for the time of a satellite pass, predictions based on ray tracing could not be expected to agree precisely with real atmospheric effects on the satellite signal. A balloon gives a profile of the refractivity that we have assumed to be vertical, but the ascent is in fact not vertical. Also, we are not able to take into account irregularities such as clouds and updrafts. The idea of a "layered" atmosphere is an approximation, while the satellite signal traverses the real atmosphere. Thus use of the model with navigation data provides the acid test. As long as use of the model results in any systematic navigation errors, further improvement should be possible.

#### ACKNOWLEDGMENT

The collaboration of Harry K. Utterback in developing the ray-tracing program and making the numerical studies based on it is acknowledged with appreciation. The navigation program that was used in the later section of the work was developed by the Analysis and Computation Group of the Space Development Department of this Laboratory. Thanks are due to L. Lee Pryor for making special modifications in the program and handling the computations involved.

# REFERENCES

1. E. K. Smith, Jr., and S. Weintraub, "The Constants in the Equation for Atmospheric Refractive Index at Radio Frequencies," Proc. I.R.E., Vol. 41, No. 8, August 1953, pp. 1035-1037.
2. H. S. Hopfield, "Two-Quartic Tropospheric Refractivity Profile for Correcting Satellite Data," J. Geophys. Res., Vol. 74, No. 18, 20 August 1969, pp. 4487-4499.
3. H. S. Hopfield, "Tropospheric Effect on Electromagnetically Measured Range: Prediction from Surface Weather Data," Radio Sci., Vol. 6, No. 3, March 1971, pp. 357-367.
4. H. S. Hopfield, "Tropospheric Range Error Parameters: Further Studies," APL/JHU CP 015, June 1972 (also published as Goddard Space Flight Center Preprint X-551-72-285, August 1972).
5. S. M. Yionoulis, "Algorithm to Compute Tropospheric Refraction Effects on Range Measurements," J. Geophys. Res., Vol. 75, No. 36, 20 December 1970, pp. 7636-7637.
6. G. Joos, Theoretical Physics, translated by Ira M. Freeman, Hafner Publishing Co., New York, 1934.
7. J. E. Freehafer, "Geometrical Optics," Vol. 13, Chap. 2, Propagation of Short Radio Waves, D. E. Kerr (Ed.), M. I. T. Radiation Laboratory Series, McGraw-Hill Book Co., 1951, and Dover Publications, New York, 1965.
8. W. M. Smart, Text-Book on Spherical Astronomy, Cambridge University Press, Cambridge, England, 1962.
9. B. R. Bean and E. J. Dutton, "Radio Meteorology," National Bureau of Standards Monograph 92, 1 March 1966.

# INITIAL DISTRIBUTION EXTERNAL TO THE APPLIED PHYSICS LABORATORY\*

The work reported in TG 1291 was done under Navy Contract N00017-72-C-4401. This work is related to Task TIC, which is supported by Defense Mapping Agency Topographic Center, 52400.

ORGANIZATION	LOCATION	ATTENTION	No. of Copies
<b>DEPARTMENT OF DEFENSE</b>			
Defense Mapping Agency Headquarters	Washington, DC	Charles Martin	1
Defense Mapping Agency Topographic Ctr.	Washington, DC	41300	1
		52200	1
		52220	1
		52400	2
DDC	Alexandria, VA		12
<u>Department of the Navy</u>			
NAVAIRSYSCOM	Washington, DC	Library, AIR-50174	2
NAVSEASYSOM	Washington, DC	Library, SEA-09G3	2
Naval Oceanographic Office	Washington, DC	D. Des Jardins, 3541	1
Naval Research Laboratory	Washington, DC	J. Buisson, 5165	1
		L. D. Breetz	1
		L. Choy, 7112 CH	1
		R. Eisinger, 7918	1
Naval Surface Weapons Ctr.	Dahlgren, VA	DK-10	1
NAVPRO	Silver Spring, MD		1
<u>Department of the Air Force</u>			
AF Western Test Range	Vandenberg, CA	C. Bucheit	1
AFCRL, Hanscom Field	Bedford, MA	R. W. Lee	1
		E. Altschuler	1
1160th Support Group, Bolling AFB	Washington, DC	CAPT P. Gollucci	1
<u>Department of the Army</u>			
A.C.I.C. Detachment No. 1	Arlington, Va.		1
<b>GOVERNMENT AGENCIES</b>			
NASA Goddard Space Flight Center	Greenbelt, MD	J. W. Marini	1
		P. E. Schmid	1
		J. Berbert	1
		D. M. LeVine	1
		S. Gubin	1
MASA Wallops Station	Wallops Island, VA	C. D. Leitao	1
National Bureau of Standards	Boulder, CO	M. C. Thompson, Jr.	1
NOAA Geodetic Research and Development Laboratories	Rockville, MD	B. Witte	1
Smithsonian Astrophysical Observatory	Cambridge, MA	G. C. Weiffenbach	1
		C. G. Lehr	1
		M. Gaposchkin	1
		M. R. Pearlman	1
		N. C. Mathur	1
<b>SCHOOLS</b>			
New Mexico State University Physical Science Laboratory	University Park, NM	D. Martin	1
Massachusetts Institute of Technology	Cambridge, MA	I. I. Shapiro	1
University of Maryland, Department of Physics and Astronomy	College Park, MD	C. O. Alley	1
		S. K. Poultney	1
		D. G. Currie	1
		I. I. Mueller	1
Ohio State University, Department of Geodetic Science	Columbus, OH	F. A. Fajamirokun	1
University of Texas	Austin, TX	A. Tucker	1

\*Initial distribution of this document within the Applied Physics Laboratory has been made in accordance with a list on file in the APL Technical Publications Group.

# INITIAL DISTRIBUTION EXTERNAL TO THE APPLIED PHYSICS LABORATORY\*

TG 1291

-2-

ORGANIZATION	LOCATION	ATTENTION	No. of Copies
<b>CONTRACTORS</b>			
California Institute of Technology, Jet Propulsion Laboratory	Pasadena, CA	G. C. C. Chao, CPB-104 P. F. MacDoran V. J. Ondrasik R. Jaffe T. Otoshi	1 1 1 1 1
Joint Institute for Laboratory Astrophysics, University of Colorado Lincoln Laboratory, Massachusetts Institute of Technology, Millstone Hill Radar	Boulder, CO	P. L. Bender	1
Analytical Sciences Corp.	Lexington, MA	A. Freed	1
DEA Systems	Reading, MA	W. Larimore	1
Mitre Corp.	Lanham, MD	G. Kiebusinski	1
General Electric Co.	McLean, VA	B. D. Elrod	1
Interstate Electronics Corp.	Utica, NY	T. Godbey, MD 309	1
Offshore Navigation Inc.	Anaheim, CA	Tech. Library, Prolantonio	1
Satellite Positioning Corp.	Harahan, LA	E. H. Christy	1
Wolf Research and Development	Encino, CA	D. Ozdes	1
Magnavox Corp.	Riverdale, MD		1
Aerospace Corp.	Torrance, CA	T. Stansell	1
	El Segundo, CA	H. M. Wachowski	1
	Los Angeles, CA	S. Leonard	1
	Dallas, TX	J. R. Hoelzel	1
	Seattle, WA	W. G. Tank	1
Collins Radio Co.			
Boeing Scientific Research Lab.			
Honeywell Inc., Gov't and Aeronautical Products Division	Meaneapolis, MN	R. J. Kell, Mail Sta. A3607	1
Systems Group of TRW Inc., Washington Operations	Washington, DC	W. H. Lewellen	1
Rand Corp.	Santa Monica, CA	J. L. Bower	1
RCA	Morristown, NJ	R. Mitchell	1
<b>FOREIGN</b>			
Geodetic Survey of Canada	Ottawa, Canada	J. D. Boal J. Kouba H. E. Jones	1 1 1
Atlantic Oceanographic Lab., Bedford Institute	Dartmouth, Nova Scotia, Canada	D. Wells	1
York University, Faculty of Science	Downsview, Ontario, Canada	R. B. Langley	1
University of New Brunswick, Department of Surveying Engineering	Fredericton, New Brunswick, Canada	M. M. Nassar	1
National Research Council of Canada, Division of Physics	Ottawa, Canada	J. Saastamoinen	1
Canadian General Electric Co. Research Dept.	Toronto, Ontario, Canada	M. R. Holmes	1
Brigadier G. Bomford	Sutton Courtenay, Oxon, England		1
Centre National d'Etudes des Télécommunications	Issy-les-Moulineaux, France	A. E. Azoulay	1
Centre National d'Etudes Spatiales	Brétigny sur Orge, France	F. Mouel M. P. Guerit P. Paquet P. Wilson K. Nottarp	1 1 1 1 1
Observatoire Royal du Belgique	Brussels, Belgium		
Institut für Angewandte Geodäsie	Frankfurt, Germany		
Astronomical Institute of the Czechoslovak Academy of Sciences	Ondrejov, Czechoslovakia	M. Prokeš	1
Meteorological Service, Division for Research	Bet Dagen, Israel	A. Manes	1
National Physical Laboratory, Radio Propagation Unit	New Delhi, India	Y. V. Semayajulu	1
National Physical Laboratory, Radio Science Division	New Delhi, India	S. B. S. S. Sarma	1
Ministry of Defense, Himalayan Radio Propagation Unit	Rajpur, Dehra Dun, India	E. Bhagiratha Rao	1
Space Applications Center, Geodesy Section (RSA)	Jodhpur Tekra, Ahmedabad, India	M. R. Sivaraman	1
National Mapping	Canberra City, Australia	B. P. Lambert	1

\*Initial distribution of this document within the Applied Physics Laboratory has been made in accordance with a list on file in the APL Technical Publications Group.

# INITIAL DISTRIBUTION EXTERNAL TO THE APPLIED PHYSICS LABORATORY\*

TG 1291

-3-

ORGANIZATION	LOCATION	ATTENTION	No. of Copies
FOREIGN (cont'd)			
University of New South Wales, School of Surveying	Kensington, N.S.W., Australia	A. Stolz	1
Weapons Research Establishment, Space Research Group	Adelaide, S.A., Australia	I. D. Lloyd	1
Australian Army Staff	Washington, DC	K. J. W. Lynn	1
		LT D. McLuskey	1

\*Initial distribution of this document within the Applied Physics Laboratory has been made in accordance with a list on file in the APL Technical Publications Group.